CNIC-01440
HUT-0001

快速托卡马克红外辐射测温仪

FAST IR DIODES THERMOMETER FOR TOKAMAK

中 国 核 情 报 中 心
China Nuclear Information Centre

CNIC-01440
HUT-0001

快速托卡马克红外辐射测温仪*

陈湘波
（合肥工业大学电气工程学院, 230009）

摘　要

描述了一个用于托卡马克装置上的快速红外测温仪。该诊断仪由 30 路快速红外二极管阵列组成，系统经实验定标后确认：时间响应为 0.5 μs；空间分辨率为 10 mm；温度测量精度小于 5 ℃；测量范围 250～1200 ℃。能给出所测第一壁在等离子体大小破裂情况下时空的两维分布，并能给出在破裂时第一壁温度百分之一的温度变化量。为托卡马克在破裂时壁温的快速变化及能量沉积过程提供了有力的测量手段。

*国家自然科学基金资助项目，资助号：19975063。

Fast IR Diodes Thermometer for Tokamak*

CHEN Xiangbo
(Hefei University of Technology, 230021)

ABSTRACT

A 30 channel fast IR pyrometry array has been constructed for tokamak, which has 0.5 μs time response, 10 mm diameter spatial resolution and 5 ℃ temperature resolution. The temperature measuring range is from 250 ℃ to 1200 ℃. The two dimensional temperature profiles of the first wall during both major and minor disruptions can be measured with an accuracy of about 1% measuring temperature, which is adequate for tokamak experiments. This gives a very useful tool for the disruption study, especially for the divertor physics and edge heat flux research on tokamak and other magnetic confinement devices.

*This work was supported by the project of National Natural Science Foundation of China (19975063).

INTRODUCTION

The tokamak configuration is the most favored approach for the confinement of nuclear fusion plasma using magnetic field. But the tokamak suffers from three main limitations at present: disruption, pulsed operation and low β values. For disruption study, it is very important to know the temperature profiles across the limiter during disruptions. The determination of the surface temperature is difficult owing to the presence of plasma, the high electrical potentials and the need not to contaminate of the surface. Infrared (IR) radiometry is a non-contactive method that overcomes the mentioned difficulties and can achieve high accuracy[1, 2]. Since the time scale of major disruption is a few tens of microseconds, for the particular purpose of disruption research, the CCD camera which is commonly used to measure the limiter temperature is not fast enough because of its long time response (20 ms) [3, 4]. So a fast radiometry with 10 μs time response is required.

The base of radiometry is Planck's law that governs the emission of radiation by blackbody:

$$M(\lambda,T)=C_1/\lambda^5(\mathrm{e}^{C_2/\lambda T}-1) \tag{1}$$

For non-ideal blackbody objects, Eq. 1 is modified as follow:

$$M(\lambda,T)=\varepsilon(\lambda,T)C_1/\lambda^5(\mathrm{e}^{C_2/\lambda T}-1) \tag{2}$$

Where T is the temperature (℃), λ is the wavelength (μm), C_1 = 3.7403×10^4 W • μm/cm^2 and C_2= 14384 μm • ℃ are the first and second radiation constants. $\varepsilon(\lambda, T)$ is the emissivity of the object which depends on the wavelength, temperature and the polarization of radiation. It is difficult to establish accurately the emissivity of limiter since it changes with the wall conditions under different discharges. For an object whose emissivity is similar to "greybody" radiation, the ratio of the intensities of radiation at two different wavelengths is independent of the emissivity. For these reasons, two-color high speed pyrometry[5～7] is chosen for accurate temperature measurement.

1 PRACTICAL CONSIDERATION

Two-color pyrometry is based on the measurement of the spectral radiance ratio at two wavelengths. According to Eq. 2:

$$Q=\frac{M(\lambda_1,\,T_1)}{M(\lambda_2,\,T_2)}=\frac{\varepsilon(\lambda_1,\,T_1)C_1/\lambda_1{}^5(\mathrm{e}^{C_2/\lambda_1 T}-1)}{\varepsilon(\lambda_2,\,T_2)C_1/\lambda_2{}^5(\mathrm{e}^{C_2/\lambda_2 T}-1)}=(\frac{\lambda_2}{\lambda_1})^5\exp\left(\frac{C_2}{\lambda T}\right) \tag{3}$$

Where $\frac{1}{\lambda}=\frac{1}{\lambda_2}-\frac{1}{\lambda_1}$

In order to achieve the greatest accuracy in the determination of temperature, measurements should be made where the radiance has the steepest variation with temperature. This can be found by differentiating Eq. 2, first with respect to T and then with respect to λ. In the limit where exp ($C_2/\lambda T$) $\gg$1, the result is:

$$\frac{\mathrm{d}^2 M}{\mathrm{d}\lambda \mathrm{d}T} = \frac{C_1 C_2 \exp(-C_2/\lambda T)}{\lambda^7 T^2}\left[-6+\frac{C_2}{\lambda T}\right]=0 \tag{4}$$

The wavelength of maximum contrast is given by

$$\lambda_{\max} = C_2/6T \tag{5}$$

Since we need a system which can measure both minor and major disruption processes, the temperature range of limiter can be rather wide. The temperature of limiter is assumed to be 300 ℃ during minor disruption and 1200 ℃ during major disruption on tokamak. It is impossible to get accurate temperature measurement between these ranges using one pair of fixed wavelengths. So we have chosen a few pairs of wavelengths to measure different temperature ranges.

Measurement of an accurate temperature of limiter depends on a few considerations: the choice of wavelength bands, the accuracy to which the emissivity value is known, the emission of non-thermal line radiation by the plasma and absorption bands in the optical path, selection of optical components, detectors and so on. The two-color system of pyrometry has been used previously in other fields [1, 2]. The following rules are important for accurate temperature measurement:

(1) The validity of graybody assumption for the wavelength intervals involved should be verified, in other words, choose the wavelength range for which the object's emissivity doesn't change rapidly.

(2) Discrete narrow band filters for the two-color system is preferred.

(3) The filter transmittance range should not overlap.

(4) The simplest optical arrangement should be chosen in order to make the calibration easier.

Following these considerations, the layout of whole system is shown as Fig. 1. Bifurcation IR fiber optics were chosen to transmit the radiation from the target to prevent loss from the vapor absorption band and to make the system very simple. By changing the support plate of the viewing optics, the system can be easy of accessing different points of limiter without the need of a vacuum break.

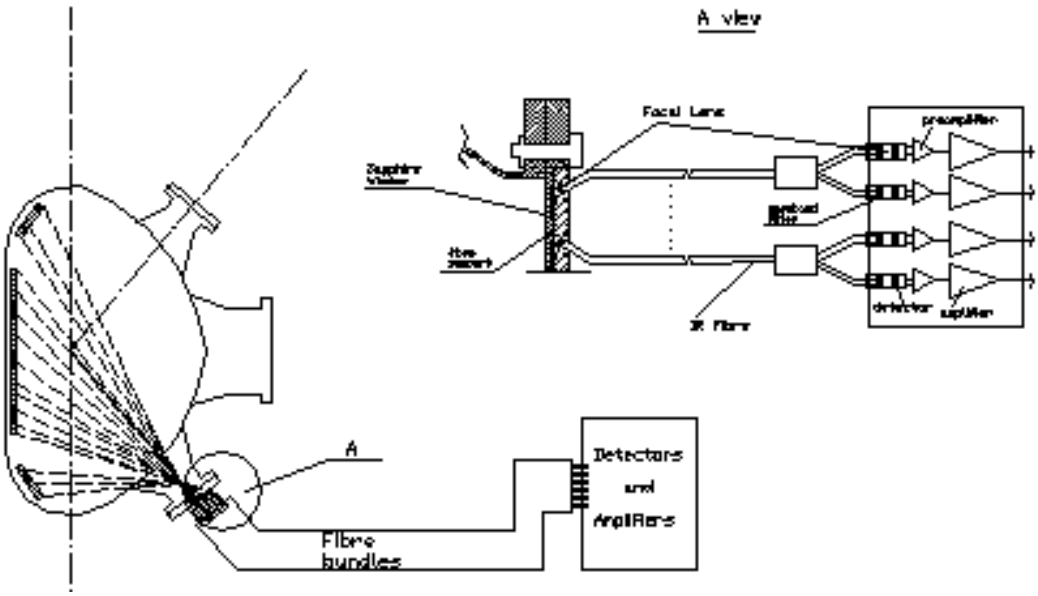

Fig. 1 The layout of the fast IR thermometry for tokamak

Room temperature InAs detectors were selected with adequate sensitivity, low noise level and low price. The whole system consists of a 30 channels pyrometry array which can give both toroidal and poloidal temperature profiles of limiter with wide bandwidth frequency response (≥2 MHz), the flexibility to observe different points on limiters and good accuracy of temperature for 3 different temperature ranges.

2 THEORETICAL ANALYSIS OF THE SYSTEM

2. 1 Performance at different wavelengths

As mentioned above, in order to achieve better accuracy in the determination of temperature, measurement should be made where the radiance has steeper variation. In general, Eq. 3 is nonlinear with temperature. For each chosen filter bandwidth, however, there is a pair of wavelength for which the ratio response is nearly linear over the particular temperature range. The linear response is very important for the calibration. Since our purpose is to measuring the temperature profile during both major and minor disruptions, during which limiter will reach different temperatures, three ranges of temperature were selected. The ratio response has maximum slope in the vicinity of this temperature and maximum sensitivity could be obtained to small changes in temperature. By carefully choosing the different wavelength bandwidth and combination of wavelength, three pairs of filters were selected with a reasonable linear range. Using the known detector's responsivity, required signal to noise ratio,

ratio of radiance at two different wavelengths and required accuracy on emissivity and so on, these three sets of filters chosen for different temperature range are as following:

(1) $\lambda_1 = 1.6\ \mu m \pm 0.16\ \mu m$ bandwidth (BW), $\lambda_2 = 2.2\ \mu m \pm 0.22\ \mu m$ BW, for $T_s \geqslant 600℃$;

(2) $\lambda_1 = 2.2\ \mu m \pm 0.22\ \mu m$ BW, $\lambda_2 = 2.6\ \mu m \pm 0.20\ \mu m$ BW, for $T_s = 300 \sim 700\ ℃$;

(3) $\lambda_1 = 2.7\ \mu m \pm 0.5\ \mu m$ BW, $\lambda_2 = 3.3\ \mu m \pm 0.50\ \mu m$ BW, for $T_s = 100 \sim 400\ ℃$.

The 1.6 and 2.2 μm set has a linear temperature range from 500 ℃ to 1400 ℃. The range for 2.2 and 2.6 μm is 300～600 ℃. The 2.7 and 3.3 μm set has the linear range 50～400 ℃ that is shown in Fig. 2.

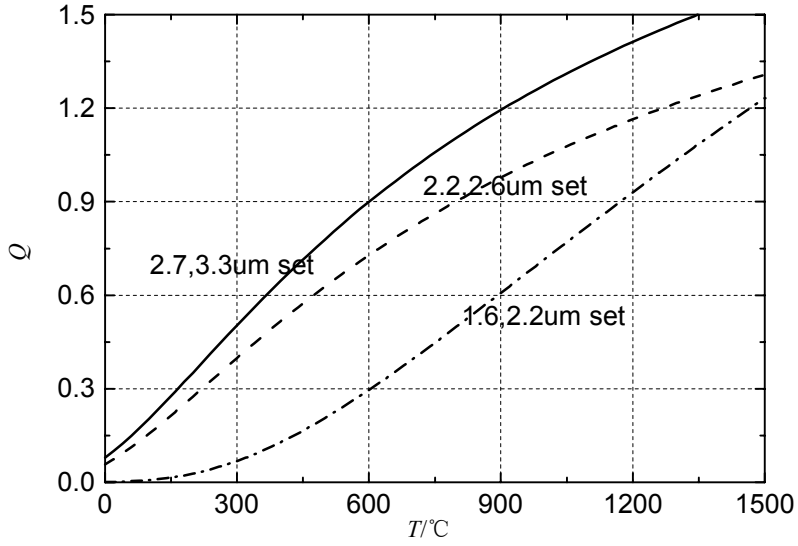

Fig. 2 Ratio of radiance at different wavelengths

2. 2 Influence of target condition

The two-color system is based on the graybody assumption. But the limiter's emissivity does change with the wavelength that will introduce some inaccuracies in the absolute temperature measurement. If Eq. 3 is differentiated with respect to the ratio of emitance, the results is

$$\frac{\mathrm{d}R}{R} = \frac{C_2(\lambda_2 - \lambda_1)}{\lambda_1 \lambda_2 T} \frac{\mathrm{d}T}{T} \tag{6}$$

Where $R = \varepsilon(\lambda_1)/\varepsilon(\lambda_2)$. Examination of this equation shows that the ratio must be known to accuracy less than the desired temperature accuracy. Fig. 3 shows the allowed range of emittance for 1% temperature accuracy for three pairs of

wavelengths. The ratios d*R*/*R* for graphite are about 10% for the 1.6 μm/2.2 μm set and 5.2% for the 2.7 μm/3.3 μm set at the room temperature. The corresponding temperature accuracy is 1.3% and 1.56%. At higher temperature (>100 ℃), the ratio of d*R*/*R* is smaller, so the temperature accuracy is within 1%.

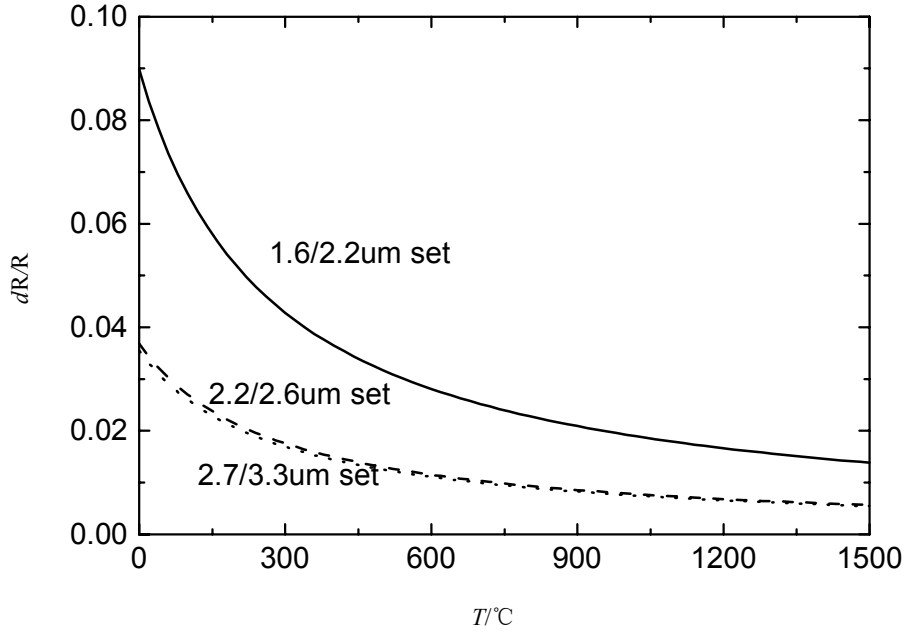

Fig. 3 Required accuracy on d*R*/*R* for 1% temperature accuracy

2. 3 Influence of Sensor's Temperature

The response curve for InAs detector has a roughly triangular shape with the steeper side towards the longer wavelengths. A temperature rise of sensor causes a shift to the left of the steep side thus decreasing the cut-off wavelength. At the same time, the other side falls, decreasing the sensitivity. The opposite happens when the sensor's temperature decreases. As shown in Fig. 4, it is clear that the sensor temperature variation causes the effective wavelengths to shift in opposite directions, introducing some inaccuracies in the temperature determination. A thorough analysis of error is complicated and we prefer to evaluate this by experimental calibration. According to other works in this field, sensor temperature control is particularly critical in two-color pyrometry. For 1% temperature accuracy measurement, the change of sensor temperature must be kept within 2 ℃.

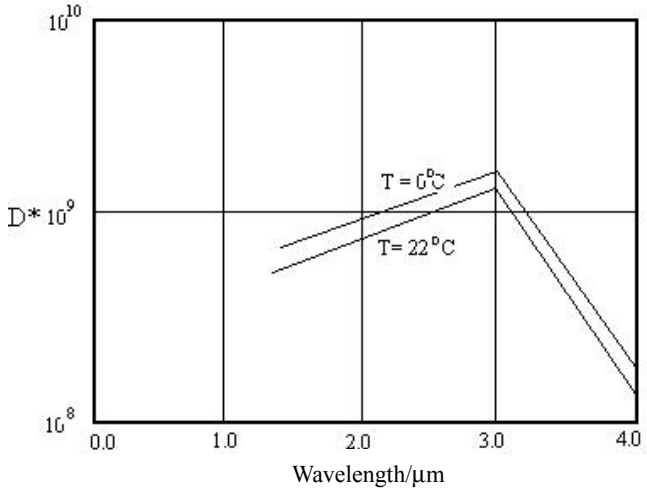

Fig. 4 Detectivity VS wavelength for J12 InAs detector

3 CALIBRATION

In practice, the detector output is not as simple as the result given by Eq. 2. For each wavelength band, the signal is of the form:

$$S = k\int_0^{\infty} \lambda^{-5} \exp(C_2/\lambda T)\tau(\lambda)\sigma(\lambda)\mathrm{d}\lambda \tag{7}$$

Where $\tau(\lambda)$ is the transmittance of whole optical system, $\sigma(\lambda)$ is the detector spectral responsivity, and k is a parameter which includes the C_1, a geometrical factor and the gain of the amplifier. Within the limit of detector linearity, k is a constant. For a narrow band filter, Eq. 7 can be simplified as:

$$S = k\lambda_1^{-5} \exp(C_2/\lambda_1 T)\tau(\lambda_1)\sigma(\lambda_1)\Delta\lambda \tag{8}$$

This makes calibration simpler.

Under this assumption, the flux ratio is equal to the signal ratio:

$$Q = \frac{S_1}{S_2} = \frac{\int_{\lambda_1} k\varepsilon\lambda^{-5} \exp(C_2/\lambda T)\tau(\lambda)\sigma(\lambda)\mathrm{d}\lambda}{\int_{\lambda_2} k\varepsilon\lambda^{-5} \exp(C_2/\lambda T)\tau(\lambda)\sigma(\lambda)\mathrm{d}\lambda} = \frac{k_1\varepsilon_1\lambda_1^{-5} \exp(C_2/\lambda_1 T)\tau(\lambda_1)\sigma(\lambda_1)\Delta\lambda_1}{k_2\varepsilon_2\lambda_2^{-5} \exp(C_2/\lambda_2 T)\tau(\lambda_2)\sigma(\lambda_2)\Delta\lambda_2} \tag{9}$$

For the particular narrow bandwidth filters (Here refer to 1.6/2.2 μm and 2.2/2.6 μm), the $\varepsilon_1 k_1 \tau_1 \sigma_1 / \varepsilon_2 k_2 \tau_2 \sigma_2$ should be constant. Then Eq. 9 becomes:

$$Q = \frac{\varepsilon_1 k_1 \tau_1 \sigma_1}{\varepsilon_2 k_2 \tau_2 \sigma_2}\left(\frac{\lambda_2}{\lambda_1}\right)^5 \exp\left[\frac{C_2}{T}\left(\frac{1}{\lambda_2} - \frac{1}{\lambda_1}\right)\right] = A_n \exp(B_n/T) \tag{10}$$

where $A_n = \frac{\varepsilon_1 k_1 \tau_1 \sigma_1}{\varepsilon_2 k_2 \tau_2 \sigma_2}\left(\frac{\lambda_2}{\lambda_1}\right)$, $B_n = C_2\left(\frac{1}{\lambda_2} - \frac{1}{\lambda_1}\right)$ are constants.

But to the passband filters (Here refer to 2.7/3.3 μm with 0.5 μm BW), the Eq. 8 is not valid, we have to use the Eq. 7. Now we define the effective wavelength λ_e as:

$$S = k\int_0^\infty \lambda^{-5} E(\lambda)\exp(C_2/\lambda T)\tau(\lambda)\sigma(\lambda)\mathrm{d}\lambda$$

$$= k\lambda_e^{-5} E(\lambda_e)\exp(C_2/\lambda_e T)\tau(\lambda_e)\sigma(\lambda_e) \qquad (11)$$

Generally, $1/\lambda_e$ fits with very small derivation in a linear function of $1/T$ (T in ℃):

$$\frac{1}{\lambda_e} = a + \frac{b}{T} \qquad (12)$$

Where a and b are the constants. The two-color pyrometry measures signal ratio:

$$Q = \frac{\phi(\lambda_{e2})}{\phi(\lambda_{e1})}\left(\frac{\lambda_{e1}}{\lambda_{e2}}\right)^5 \exp\left(\frac{C_2}{T\lambda_e}\right) \qquad (13)$$

Where $\phi(\lambda_e) = E(\lambda_e)\tau(\lambda_e)\sigma(\lambda_e)$, λ_e is the effective equivalent wavelength:

$$1/\lambda_e = 1/\lambda_{e2} - 1/\lambda_{e1}$$

According to Eq. 12, λ_e may also be written as:

$$\frac{1}{\lambda_e} = e + \frac{d}{T} \qquad (14)$$

Commonly, we also have:

$$\left(\frac{\lambda_{e1}}{\lambda_{e2}}\right)^5 = \left(\frac{a + b/T}{a' + b'/T}\right)^5 \cong \left(\frac{a}{a'}\right)^5 \left(1 + \frac{5(a'b - ab')}{aa'T}\right) \qquad (15)$$

ϕ_1/ϕ_2 is fairly constant, so we have:

$$\frac{\phi(\lambda_{e2})}{\phi(\lambda_{e2})}\left(\frac{\lambda_{e1}}{\lambda_{e2}}\right)^5 = f + \frac{g}{T} \qquad (16)$$

Putting Eq. 14, 16 into Eq. 12 and neglecting higher orders of small quantities, we can get:

$$T = \frac{B_n}{\ln Q - A_n} + C_n \qquad (17)$$

where e, d, f, g, A_n, B_n, C_n are constants.

The calibration consists of setting different T_1, T_2, … , T_n, getting a number of corresponding ratios Q_1, Q_2, … , Q_n and finding the coefficients A_n, B_n, C_n through least square method.

A WK—9C blackbody source was used for the calibration. It has a temperature range 0～1200 ℃. Table 1 to 3 are the calibration results. Table 1 and 2 use Eq. 10. Table 3 uses Eq. 17. The maximum error bar is 1.5% that is a bit large than expected. The reason for this could be the sensor temperature change during the calibration, the

instability of source temperature and inaccuracy on data reading. If the temperatures of the sensor and source are kept constant and more accurate data acquisition system is used, then better accuracy could be achieved. The temperature resolution measured is about 5 ℃.

Table 1 The calibration results for the first set filters

T_s/℃	S_1/1.6 μm	S_2/2.2 μm	T_m/℃	$T_s - T_m$/℃	Error
1000	10.5	62.6	1002.6	−2.6	−0.26
1025	12.6	71.3	1021.4	3.6	0.35
1050	15.8	83.2	1054.2	−4.2	−0.40
1075	17.7	88.3	1078.5	−3.5	−0.32
1100	20.4	98.3	1096.3	3.7	0.33
1125	23.0	105.5	1121.4	3.6	0.32
1150	25.4	110.0	1152.0	−2.0	−0.18
1175	27.6	114.4	1176.2	−1.2	−0.10
1200	29.4	117.4	1196.8	3.2	0.27

Table 2 The calibration results for the second set filters

T_s/℃	S_1/2.2 μm	S_2/2.6 μm	T_m/℃	$T_s - T_m$/℃	Error/%
600	4.1	2.7	605.1	−5.1	−0.9
650	5	2.9	655.2	−5.2	−0.8
700	7.4	3.9	698.8	1.2	0.2
750	10.3	4.9	752.3	−2.3	−0.3
800	13.7	6.1	794.6	5.4	0.7
850	18.9	7.8	847.3	2.7	0.3
900	24.8	9.5	897.7	2.3	0.3
950	29.8	10.8	944.4	5.6	0.6
1000	39.8	13.5	1005.2	−5.2	−0.5

As mentioned above, the sensor's temperature is very important. If the sensor temperature changes from 22.5 ℃ to 25.5 ℃ and we still use the coefficients A_n, B_n, C_n at 22.5 ℃, this would introduce maximum 0.5% error bar to temperature measurement. So the change of sensor temperature must be kept within 2 ℃.

The change of detector responsivity with its temperature was also measured and

is shown as Fig. 5. We can see the sensitivity at 0 ℃ increases by nearly a factor of 3 compared to that at 20 ℃. By selecting a suitable cooling system (set the temperature at 0 ℃, for example), the lowest measurable temperature can be reduced down to 250 ℃ with 3 ℃ temperature resolution.

Table 3 The calibration results for the third set filters

T_s/℃	S_1/2.7 μm	S_2/3.3 μm	T_m/℃	$T_s - T_m$/℃	Error/%
350	1.15	1.95	355.4	−5.4	−1.5
400	1.65	2.56	403.2	−3.2	−0.8
450	2.53	3.67	454.1	−4.1	−0.9
500	3.82	5.2	499.3	0.7	0.1
550	5.52	7.18	549.6	0.4	0.1
600	7.86	9.67	605.2	−5.2	−0.9
650	10.9	12.9	655.2	−5.2	−0.8
700	14.1	16	705.3	−5.3	−0.8

The time response of whole instruments was measured using a 2 mW HeNe laser that is driven by a 1 MHz step function generator. The input has a rise time of less than 0.1 μs. With this input, the output was observed to have a rise time (10%～90%) of 0.45 μs. So the frequency bandwidth of whole system is about 2 MHz.

The spatial resolution was measured by using the blackbody source. The channel-to-channel separation on the limiter is designed to be about 20 mm, and each channel views a sport of 10 mm in diameter. There is no measurable cross talk between channels. By choosing the lower angle port, the central limiter, top divertor plates can be viewed by the system that is shown on Fig.1.

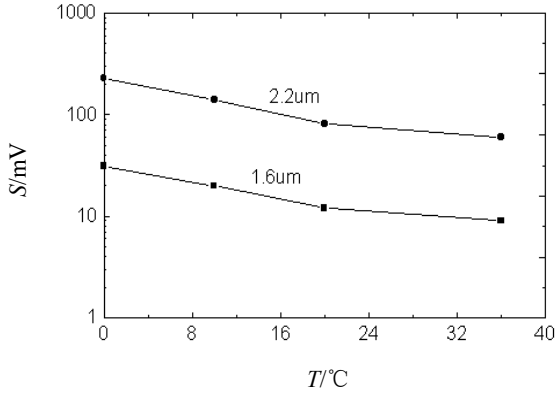

Fig. 5 The detector responsivity with its temperature

4 CONCLUSION

A 30 channel fast IR pyrometry array has been constructed which has 0.5 μs time response, 10 mm diameter spatial resolution and 5 ℃ temperature resolution. The temperature range is from 250 ℃ to 1200 ℃. The two-dimensional temperature profiles of the limiter during both major and minor disruptions can be measured with about 1% temperature measuring accuracy that is adequate for tokamak experiments. This gives a very useful tool for disruption study, especially for the divertor physics and edge heat flux research on tokamak.

REFERENCES

1 Cezairliyan A. Temperature: Its Measurement and Control in Science and Industry. (Edited by H. H. Plumb), (Instrument Society of America, Pittsbugh, 1972), Vol. 4, Part 1. 657

2 Cezairliyan A, Babelot J F, Magill J, Ohse R W. Radiation Thermometry. (Edited by D. P.. DeWitt and G. D. Nutter) (Wiley, New York, 1989), P529

3 Taylor T, Brooks N H, McMahon T R, Pipkins J F, Ioki K. BAPS, 1981, 26: 876

4 Bush C E, Foster O L, Ketterer H E, Overbey D R. BAPS, 1980, 25: 975

5 Ulrickson M, Pearson G G. Journal of Nuclear Materials, 1982, 111～112: 91

6 Albert Z, Abraham K. Applied Optics, 1991, 30: 660

7 Cezairliyan A, Chang R F, Foley G M, Miiler A P. Rev. Sci. Instrum., 1993, 64: 158

陈湘波：合肥工业大学电气工程学院助理研究员。1983 年毕业于华中理工大学。

CHEN Xiangbo: Associate Researcher of Institute of Electrical Engineering, Hefei University of Technology. Graduated from Huang Zhong University in 1983.